Available online at www.sciencedirect.com
ScienceDirect
Journal of Power Sources 171 (2007) 1033–1039
JOURNAL OF POWER SOURCES
www.elsevier.com/locate/jpowsour

High-power nickel/metal-hydride battery using new micronetwork substrate: Discharge rate capability and cycle-life performance

Masaru Yao [a,*], Kazuki Okuno [b], Tsutomu Iwaki [a], Shigeo Tanase [a], Keizo Harada [b], Masahiro Kato [b], Katsuji Emura [b], Tetsuo Sakai [a,*]

[a] *National Institute of Advanced Industrial Science and Technology (AIST), Kansai Center, 1-8-31 Midorigaoka, Ikeda, Osaka 563-8577, Japan*
[b] *Sumitomo Electric Industries, Ltd., 1-1-1, Koyakita, Itami, Hyogo 664-0016, Japan*

Received 11 April 2007; received in revised form 12 June 2007; accepted 27 June 2007
Available online 1 July 2007

Abstract

A new positive substrate for high-power nickel/metal-hydride (Ni/MH) battery was designed and prepared based on a nonwoven cloth technique. For the substrate, the amount of plated nickel was reduced to less than half compared with the conventional foam-type substrate, and the manufacturing process was simplified, which lowers the manufacturing cost of the substrate. The sub-C size cylindrical sealed cell using the developed substrate exhibited superior high-rate discharging capability to the cell using the foam-type one in spite of the reduction in the amount of plated nickel due to the characteristic three-dimensional micronetwork structure of the developed substrate. In addition, the prepared cell exhibited a long cycle-life of more than 2000 cycles at 25 °C. A hybrid electric vehicle (HEV) mode cycle test consisting of multiple pulse patterns was also performed on the cell at 45 °C, and the cell remained more than 85% power of the initial value even after 100,000 cycles (driving distance: ca. 300,000 km). The developed micronetwork substrate was revealed to satisfy both high-power output and long cycle-life.
© 2007 Elsevier B.V. All rights reserved.

Keywords: Nickel/metal-hydride battery; Positive electrode; Hybrid electric vehicle; High-power application

1. Introduction

During more than 100-year history of alkaline secondly batteries, these batteries have continued progress, and are widely used as power sources of familiar electric devices, nowadays. Among the alkaline secondly batteries, nickel/metal-hydride (Ni/MH) battery has been prevalent from the viewpoint of its output capability, life, reliability, cost, and low-polluting characteristic. In addition, the usage as the power sources for hybrid electric vehicles (HEVs) has been recently growing [1–5]. As the HEVs exhibit high gas mileage, the recent oil prices soaring accelerate their purchase; however, they are still expensive compared with usual gasoline-powered vehicles. For the further expansion of the market, the cost reduction and further improvement of the power for Ni/MH battery are strongly required.

Many studies have been reported on the Ni/MH batteries for HEV usage; however, the studies on a substrate are only a few [6–8]. For the positive electrode, foam-type nickel substrates are commonly used nowadays to address the requirements of high power and high capacity [6], and the remaining problem for the positive substrate is its high manufacturing cost. One of the approaches for lowering the cost of the substrate is the reduction in the amount of nickel; however, it often decreases the mechanical strength of the resultant electrode. In order to develop a nickel-reduced substrate having enough strength as the electrode, we have focused on a nonwoven cloth made of polyolefin fibers [9]. New substrate was manufactured by plating nickel onto a newly designed nonwoven cloth that has a characteristic three-dimensional micronetwork structure. Since the inner fibers add enough strength to the electrode, the amount of nickel of the new micronetwork substrate could be reduced to half, compared with that of the conventional foam-type substrate.

In this paper, the high-rate discharging capability of the new micronetwork substrate was compared with the conventional foam-type substrate, by using sub-C size cylindrical sealed cells.

* Corresponding authors. Tel.: +81 72 751 9611; fax: +81 72 751 9623.
E-mail addresses: m.yao@aist.go.jp (M. Yao), sakai-tetsuo@aist.go.jp (T. Sakai).

0378-7753/$ – see front matter © 2007 Elsevier B.V. All rights reserved.
doi:10.1016/j.jpowsour.2007.06.211

In addition, cycle-life performances of the prepared cells were evaluated in the conventional full charge/discharge tests using the 1-C rate current. A pulse mode cycle-life test consisting of complex charge/discharge pattern was also applied for the cell considering practical applications of the micronetwork substrate for the HEV system.

2. Experimental

2.1. Manufacturing and characterization of new micronetwork substrate

New micronetwork substrate was prepared by plating nickel onto a polyolefin nonwoven cloth having a three-dimensional micronetwork structure as described in our previous paper [9]. The outline of the manufacturing process of the micronetwork substrate is as follows. An electroconductive coating was first carried out to the specially designed nonwoven cloth by the electroless nickel plating method. Then, the electroplating of nickel was performed, in which the net amount of nickel plating was adjusted to 200 g m^{-2}. The applied amount of nickel is less than half compared with the conventional foam-type substrate with nickel plating of 420 g m^{-2} (Celmet® No. 8, Sumitomo Electric Industries, Ltd., Japan), The morphology of the substrates and the resultant electrodes was examined by a scanning electron microscope (SEM, S-2150, Hitachi, Ltd., Japan), and an optical microscope (MX40, Olympus Corp., Japan). The pore size distribution was measured with a handmade porosimeter based on a bubble point technique. The surface area of each substrate was measured by Brunauer–Emmett–Teller (BET) method.

2.2. Cyclic voltammetric measurement

To estimate the property of the micronetwork substrate as the electrode, the cyclic voltammetric (CV) measurement was first applied. The working electrode was prepared in the similar composition used for the electrode of the sealed cells except for the use of poly-tetrafluoroethylene (PTFE) (Daikin Industries, Ltd., Japan) as a binder. The measurement was performed by using an electrochemical analyzer (SI 1280B, Solartron, UK) with an Hg/HgO reference electrode and a hydrogen absorbing alloy as a counter electrode. After the activation process by several cycling of the working electrodes, the voltammograms were recorded at a scan speed of 0.1 mV s^{-1}, with a potential range of 0.1–0.6 V versus the reference electrode.

2.3. Preparation and evaluation of sub-C size sealed cells

The positive electrodes for sealed cells were prepared by a paste method as follows. Cobalt compound coated $Ni(OH)_2$ powder, $Co(OH)_2$ powder (Tanaka Chemical Corp., Japan), and carboxymethylcellulose (CMC) (Daicel Chemical Industries, Ltd., Japan) were mixed thoroughly in the weight ratio of 100:7.5:0.15 with water, and the paste was loaded into each substrate (30 mm × 270 mm). These electrodes were dried and then roll-pressed to a thickness of ca. 450 μm. Each positive electrode was adjusted to have the same capacities of 2.2–2.3 Ah (ca. 550 mAh cm^{-3}). As the negative electrode, the conventional $Mm(Ni, Co, Mn, Al)_5$-type hydrogen-absorbing alloy coated on a punched metal sheet was used [8,10]. The capacity of the negative electrode was about twice as large as that of the positive electrode. The positive and negative electrodes were spirally wound together with a sulfonated polypropylene separator, and the bundle was inserted and welded to a sub-C size cylindrical case. After the welding of a cover plate to the terminal of the positive electrode, the case was filled with an electrolyte and then the cell was sealed.

The high-rate discharging capability of the prepared sub-C size sealed cells was examined by discharging at the 2-, 5-, and 10-C rates using a cut-off voltage of 0.6 V at fully charged state after an activation process consisting of several charge/discharge patterns at low-rate currents. In a pulse test, the cells were discharged for 10 s at various currents ranging from 1- to 35-C rates at the 50% state of charge (SOC).

The conventional cycle-life tests were evaluated at 25 and 45 °C using the 1-C rate current for both charge and discharge. In addition, an HEV mode cycle-life test was performed at 45 °C based on the procedure established by Japan Electric Vehicle Standard by Japan Automobile Research Institute (JARI) [11]. The HEV mode test consists of multiple charge/discharge patterns for a few seconds in which maximum charge and discharge rates were the 7- and 10-C rates, respectively. The power output was calculated from the voltage at the maximum discharge rate of the 10-C at the 50% SOC. All the charge/discharge tests were conducted using a computer-controlled charge/discharge system (BLS series, Keisokuki Center Co., Japan) equipped with a thermostatic chamber.

3. Results and discussion

3.1. Microstructure of substrate

The amount of plated nickel of the micronetwork substrate was reduced to less than half compared with that of the foam-type substrate. Besides, the micronetwork substrate has a fewer manufacturing step than the foam-type nickel substrate. Since the micronetwork substrate is made from alkaline-resistant polyolefin nonwoven cloth instead of polyurethane foam, the burring processes to remove the inner material can be omitted in manufacturing the substrate, which also leads to the cost reduction. The remaining inner fibers also work for adding enough mechanical strength required for electrodes to the substrate.

Fig. 1 shows the SEM image of the micronetwork substrate and the conventional foam-type substrate. As shown in the figure, the micronetwork substrate has a fine three-dimensional structure based on the nonwoven cloth. In addition, the micronetwork substrate has a smoother surface than the foam-type one, which could suppress the risk of short circuit during the winding of the electrodes. Fig. 2 shows the pore size distribution of each substrate measured by the bubble point technique. The maximum pore diameters exhibited by the pore size distribution of the micronetwork substrate and the foam-type one were 65 and 85 μm, respectively. Besides, the specific surface areas of both

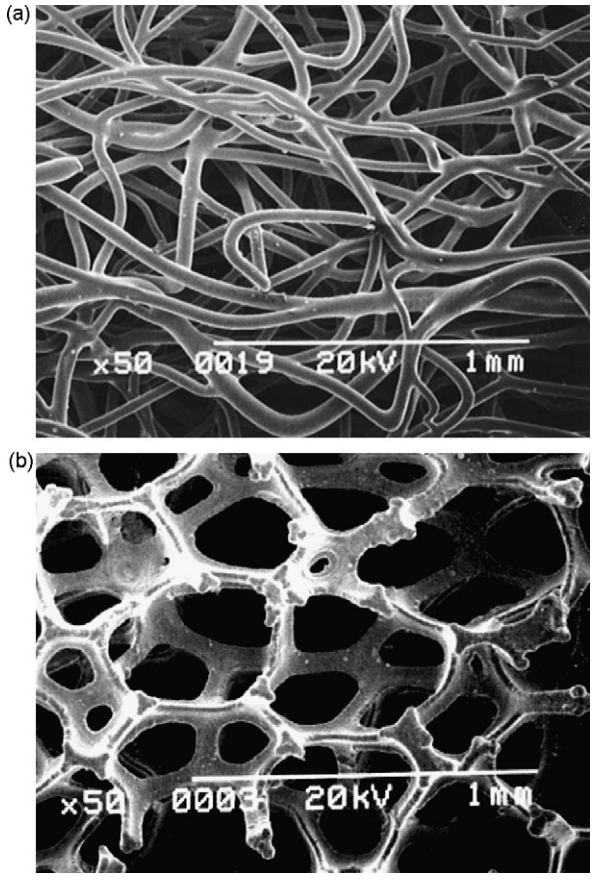

Fig. 1. SEM images of (a) new micronetwork substrate and (b) foam-type substrate.

substrates were measured by the BET method. The obtained values for the micronetwork substrate and the foam-type one were 0.52 and 0.10 $m^2\ g^{-1}$, respectively. The micronetwork substrate has about a five times larger surface area than the foam-type one. For the conventional foam-type substrate, further enhancements of the surface area and the reduction of the pore size are difficult because of the limitation in the manufacturing condition of polyurethane foam. In contrast, the pore size or the surface area of the micronetwork substrate can be easily controlled because of the characteristic flexibility of nonwoven cloths.

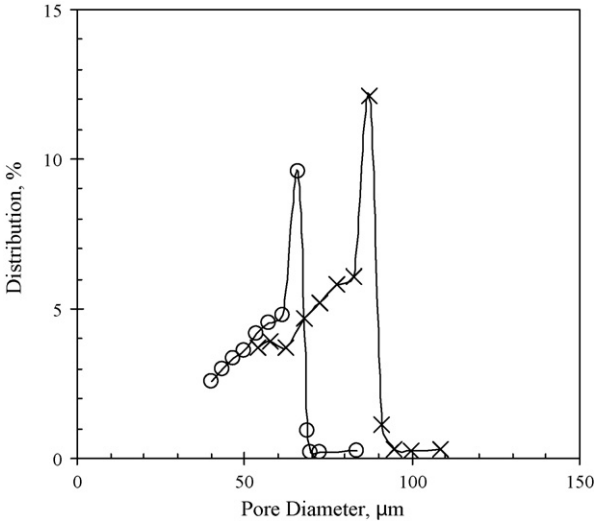

Fig. 2. Pore size distribution measured by bubble point method. (◯) New micronetwork substrate and (×) foam-type substrate.

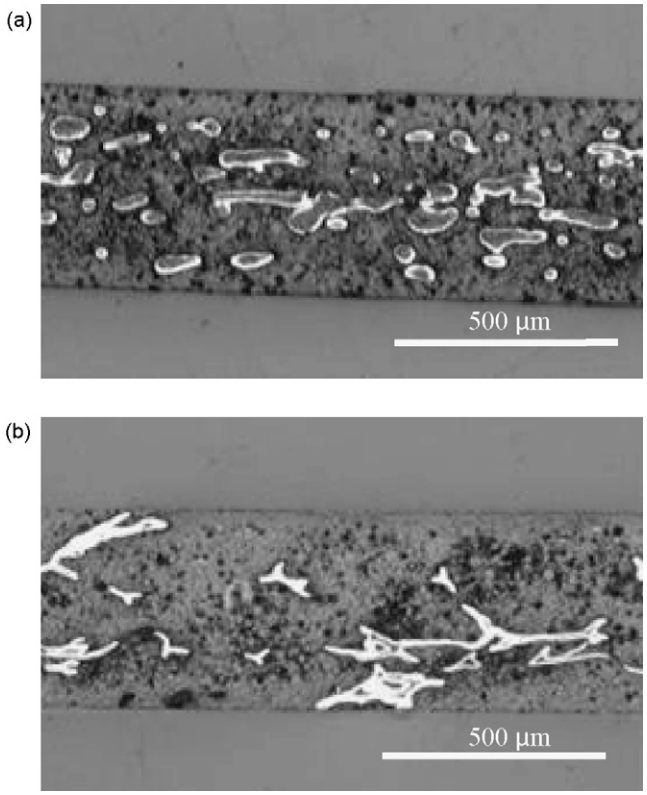

Fig. 3. Cross-sectional images of the electrodes using (a) new micronetwork substrate and (b) foam-type substrate.

Fig. 3 shows the cross-sectional images of the prepared electrodes by the optical microscope. The dark background in Fig. 3a is the filled active material and the bright ring-like parts are nickel-plating layers. The inner parts of the ring-like layers are the remained polyolefin fibers. Apparently, the nickel layer of the micronetwork substrate is thinner than that of the foam-type substrate shown in Fig. 3b, which reflects the reduction in the amount of plated nickel. In addition, the region surrounded by the nickel frameworks becomes smaller by using the micronetwork substrate with smaller pore diameter.

3.2. CV behavior of the electrodes

CV technique was applied for the electrodes prior to the battery test to estimate a preparatory charge/discharge performance of the micronetwork substrate. Fig. 4 shows the cyclic voltammograms of the electrodes using the micronetwork substrate and the conventional foam-type one. The peaks at around 0.5 and 0.25 V are ascribed to the anodic and cathodic reactions of nickel hydroxide, respectively [12]. The increasing current at around 0.6 V is due to the oxygen evolution. Interestingly, the electrode using the micronetwork substrate exhibited the larger currents at both anodic and cathodic peaks compared with those of the electrode using the foam-type one. Accord-

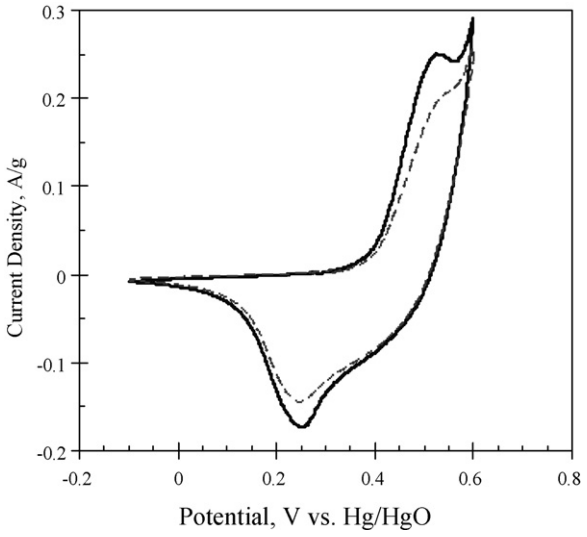

Fig. 4. Cyclic voltammograms of the electrodes using new micronetwork substrate (solid line) and foam-type substrate (broken line).

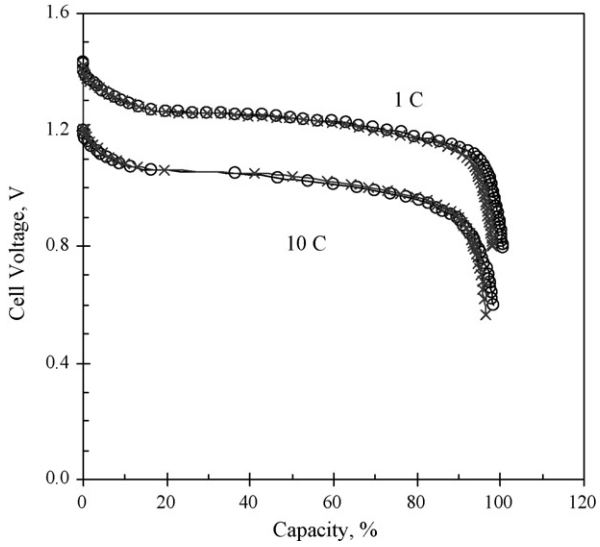

Fig. 5. Discharging curves of sealed cells at the 1- and 10-C rates. (◯) Cell using the new micronetwork substrate and (×) cell using the foam-type substrate.

ing to a theoretical study, the redox peak current is directly proportional to the surface area of the substrate as expressed in Randles–Sevcik type equation. The observed larger peak currents for the electrode using the micronetwork substrate can be ascribed to its larger surface area, since the other parameters are the same in our measurement, which implies the possibility for the superior charge/discharge capability of the micronetwork substrate.

3.3. High-rate discharge performance of cylindrical sub-C size sealed cells

In order to figure out the property of the micronetwork substrate in a practical condition, cylindrical sub-C size sealed cells were prepared, and their discharge characteristics were evaluated. In a preliminary high-rate discharging test using various micronetwork substrates, a close relationship between the substrate pore structure and the cell voltage was obtained, in which the cell using a substrate with smaller pore size provided a better rate capability than the cells using substrates with larger pore size. Fig. 5 shows the comparison of the discharging curves at the 1- and 10-C rates for the sub-C cells using the micronetwork substrate and the foam-type one. The micronetwork substrate itself has nearly twice-higher electric resistance in the in-plane direction than the foam-type substrate owing to the reduction in the amount of the used nickel. However, no obvious difference in the discharging voltages and the capacity utilities was observed even at the 10-C rate discharging. In addition, both cells exhibited almost the same internal resistances of $8 \pm 1\ \mathrm{m\Omega}$ at 1 kHz. Among resistance components of an electrode, a contact resistance between a substrate and active materials is closely related to the contact area between them. Since the micronetwork substrate has a larger surface area as described above, the contact resistance in the electrode is considered to become smaller than that of the foam-type used electrode. Therefore, the obtained discharging behavior suggests that the large surface area of the substrate will compensate the increased resistance of the substrate itself.

To examine the instantaneous high-rate discharging characteristic of each cell, a pulse-type discharging test above the 10-C rate was performed. In an HEV pattern cycle test proposed by JARI [11], the maximum discharge current at the 10-C rate is used; however, a higher discharging capability is desired for a smoother acceleration of the vehicle. Fig. 6 shows the voltage responses upon the discharging for 10 s at 50% of SOC of the cells using the micronetwork substrate and the foam-type one. The initial voltage drops seen in the figure are mainly ascribed to the ohmic loss of the cell components. During discharging at the currents of the 1- and 10-C rates, both cells exhibit the constant voltages for 10 s. At the higher rates, the voltage of the cell using foam-type substrate tends to drop during discharging; however, the cell using the micronetwork substrate exhibits almost constant voltage during discharging even at the 30-C rate. The relationship between the current and the voltage after 10 s discharge is summarized as the current–voltage (*I*–*V*) plots in Fig. 7. Both cells exhibit almost no difference at the current rates below 20-C; however, the difference becomes clear at the higher rate discharging. In the *I*–*V* plots, the behavior of the cell using the micronetwork substrate shows a linear relationship, although that of the cell using the foam-type one is deviated from the linear relationship.

The internal resistance of cells includes many components, such as ohmic resistance of consisting materials, electrochemical charge-transfer resistance, and ionic diffusion process. During the discharging at the low-rate, the first ohmic resistance is considered to be a main factor for the total internal resistance; however, the influence of other resistance components can become large at the high-rate discharge [13] and these factors relating to the electrochemical reaction cause a voltage drop during discharging [14]. In addition, the discharging current exhibits a limitation which is closely related to the surface area of the substrate in general electrode reaction, since the large

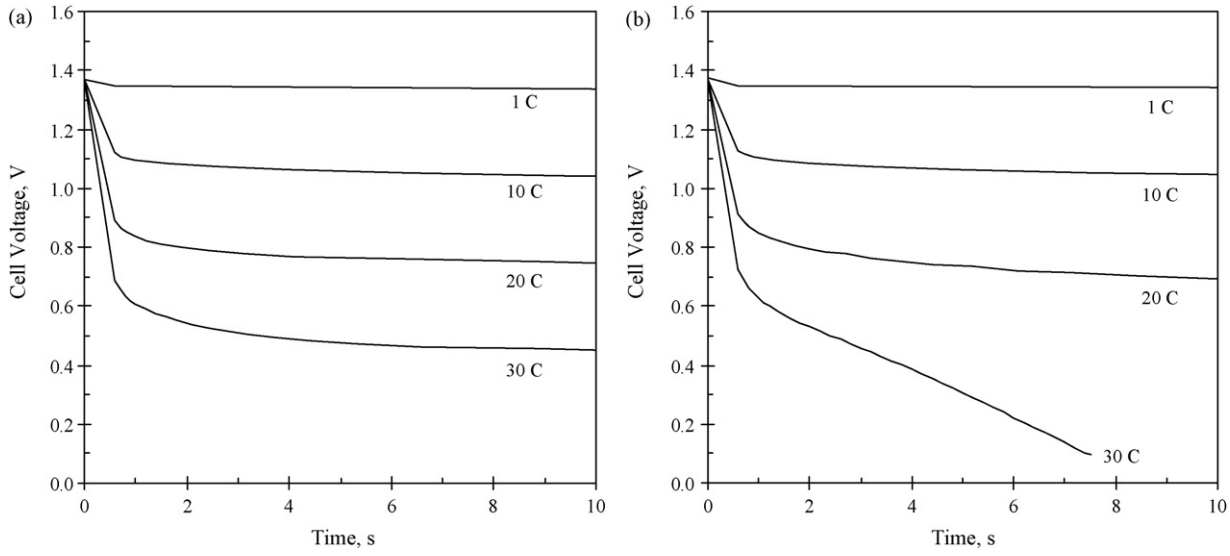

Fig. 6. Ten second discharging curves of the sealed cells at 50% SOC. (a) Cell using the new micronetwork substrate and (b) cell using the conventional foam-type substrate.

portion of electrochemical reaction occurs at the surface of the substrate. Even if an apparent current density per unit area of an electrode is equal, true current density changes depending on the surface area of the used substrate. Specifically, the true current density is inversely proportional to the surface area of the substrate. Besides, net amounts of reacting active materials at the substrate interface become large, by using a larger surface area substrate. In general, the battery voltage during discharging also depends on the concentration of reacting active materials at the surface of the current collector as derived from the Butler–Volmer equation [15,16]; therefore, a large concentration of active materials at the surface is considered to suppress a rapid voltage drop during high-rate discharging. In our case, the electrode using the micronetwork substrate has a large contact area between the current collector and the active material compared with the electrode using the conventional foam-type one, which probably contribute not only to the reduction of the contact resistance but also to the enhancement in the reactivity.

3.4. Cycle-life performance of the cell using the micronetwork substrate

The conventional charge/discharge cycle test at the 1-C rate current was carried out for the cell using the micronetwork substrate. The capacity retention of the cell at 25 °C is shown in Fig. 8. No capacity decay is observed at the cycle below 1000 cycles. The capacity began fading after that; however, the cell kept about 90% of capacity even after 2000 cycles. In the accelerated test performed at 45 °C, the prepared cell also exhibited long cycle-life, and the cell kept more than 90% of capacity retention

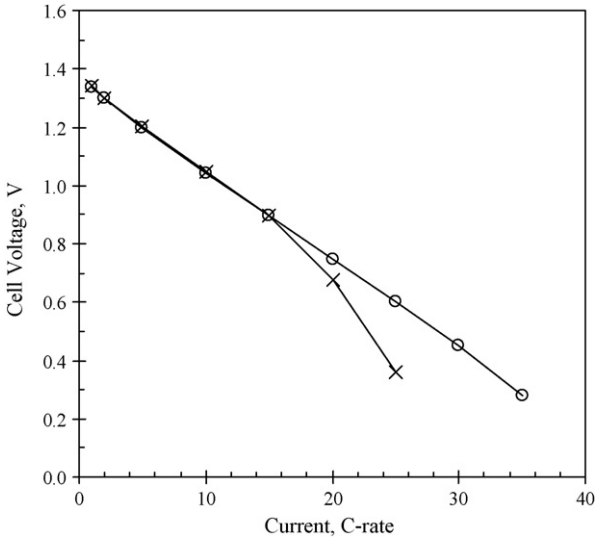

Fig. 7. Relationship between the current rate and the cell voltage after 10 s discharging at 50% SOC. (◯) Cell using the new micronetwork substrate and (×) cell using the foam-type substrate.

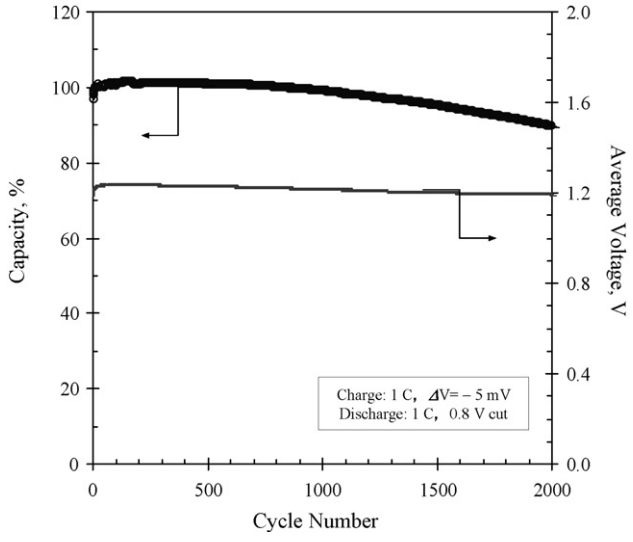

Fig. 8. Cycle-life performance of the cell using the new micronetwork substrate at 25 °C.

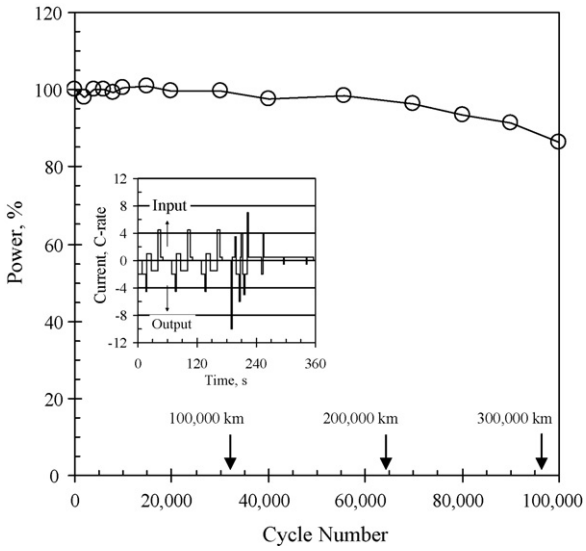

Fig. 9. HEV mode-pattern cycle performance at 45 °C for the cell using the new micronetwork substrate. The inset shows the applied charge/discharge pulse pattern [11].

after 500 cycles. At both temperatures, the average voltages did not change drastically during the long cycle. The substrate after long cycles was examined by a microscopic measurement and X-ray diffraction analysis; however, no remarkable deterioration was observed, which also implies the high tolerance of the micronetwork substrate.

Considering the application of the cell using the micronetwork substrate to the HEVs, a pulse-type test based on actual driving patterns was applied at 45 °C [11]. In the HEV mode test pattern shown in the inset of Fig. 9, one cycle corresponds to the mileage of 3.12 km, and more than 100,000 km mileage (corresponding to about 32,000 cycles) is required for the HEV battery. As seen in Fig. 9, the cell using the micronetwork substrate remained more than 85% power of the initial value even after 100,000 cycles in the HEV mode test, which corresponds to a driving distance of more than 300,000 km.

In conventional positive electrodes, some polymeric materials, such as poly-tetrafluoroethylene (PTFE) and polypropylene (PP), are often added as binders into a paste of active materials to avoid a separation of the active materials from current collectors due to the swelling of the electrode, although the addition of these binders often causes an increase in the internal resistances. In this work, these materials were not used for the cells; however, they exhibited an excellent cycle-life performance, which indicates the high retention ability of the micronetwork substrate for the active materials. The developed substrate would be used for not only familiar application as an electric power sources, but also HEV applications.

4. Conclusions

A new low-cost substrate for the positive electrode of nickel/metal-hydride battery was prepared by electrochemical plating of nickel onto polyolefin nonwoven cloth with a characteristic three-dimensional micronetwork structure, in which the amount of plated nickel was reduced to less than half compared with the conventional foam-type substrate. The substrate is manufactured in the simplified process compared with the conventional foam-type one.

The sub-C size cylindrical sealed cell using the micronetwork substrate exhibited comparable rate capability to the cell using the conventional foam-type substrate even at the 10-C rate discharging. Moreover, the cell using the micronetwork substrate exhibited superior high-rate capability to the conventional cell in the pulse discharging, although the amount of plated nickel of the substrate is only the half of that of the foam-type substrate. The micronetwork substrate has smaller pore diameter and the larger surface area than the conventional foam-type substrate; and its characteristic micronetwork structure presumably contributes to the reduction of the contact resistance and the enhancement in the reactivity of the active material at the surface of the substrate, which synergistically improves the high-rate discharge capability of the cell. Besides, the cell using the micronetwork substrate exhibited long cycle-life in the conventional charge/discharge tests, and showed a good performance in the HEV mode cycle test at 45 °C, in which the cell exhibited more than 100,000 cycles (driving distance of ca. 300,000 km). The developed substrate was revealed to have an adequate property as the positive substrate for the HEV application.

The micronetwork substrate has high flexibilities in structure, such as thickness, porosity, and pore size, compared with the conventional foam-type substrate. By designing the microstructure of the nonwoven cloths, it would lead to much more improvement of the high-power Ni/MH battery.

References

[1] N. Fujioka, M. Ikoma, K. Kanamaru, The 15th International Electric Vehicle Symposium No. 1, 1998, p. 69.
[2] T. Sakai, I. Uehara, H. Ishikawa, J. Alloys Compd. 293–295 (1999) 762–769.
[3] R.F. Nelson, J. Power Sources 91 (2000) 2–26.
[4] A. Taniguchi, N. Fujioka, M. Ikoma, A. Ohta, J. Power Sources 100 (2001) 117–124.
[5] K. Shinyama, Y. Magari, K. Kumagae, H. Nakamura, T. Nohma, M. Takee, K. Ishiwa, J. Power Sources 141 (2005) 193–197.
[6] I. Matsumoto, S. Ikeyama, T. Iwaki, H. Ogawa, Denki Kagaku 54 (1986) 159–163.
[7] M. Oshitani, H. Yufu, K. Takahashi, S. Tsuji, Y. Matsumura, J. Electrochem. Soc. 136 (1989) 1590–1593.
[8] H. Fukunaga, M. Kishimi, N. Matsumoto, T. Ozaki, T. Sakai, T. Tanaka, T. Kishimoto, J. Electrochem. Soc. 152 (2005) A905–A912.
[9] M. Yao, K. Okuno, T. Iwaki, M. Kato, K. Harada, J.J. Park, S. Tanase, T. Sakai, Electrochem. Solid-State Lett. 10 (2007) A56–A59.
[10] T. Ozaki, H.-B. Yang, T. Iwaki, S. Tanase, T. Sakai, H. Fukunaga, N. Matsumoto, Y. Katayama, T. Tanaka, T. Kishimoto, M. Kuzuhara, J. Alloys Compd. 408–412 (2006) 294–300.
[11] Japan Automobile Research Institute Standards Committee, Cycle Life Test Procedure of Sealed Nickel–Metal Hydride Batteries for Hybrid Electric Vehicles, JEVS D 716, Japan Automobile Research Institute, Tokyo, 2004.
[12] D.A. Corrigan, R.M. Bendert, J. Electrochem. Soc. 136 (1989) 723–728.

[13] A.H. Zimmerman, P.K. Effa, J. Electrochem. Soc. 131 (1984) 709–713.
[14] M. Yao, K. Okuno, T. Iwaki, M. Kato, K. Harada, J.J. Park, S. Tanase, T. Sakai, J. Electrochem. Soc. 154 (2007) A709–A714.
[15] B. Paxton, J. Newman, J. Electrochem. Soc. 144 (1997) 3818–3831.
[16] W.B. Gu, C.Y. Wang, S.M. Li, M.M. Geng, B.Y. Liaw, Electrochim. Acta 44 (1999) 4525–4541.